Electrical Power and Energy Systems 45 (2013) 271–278

Contents lists available at SciVerse ScienceDirect

Electrical Power and Energy Systems

journal homepage: www.elsevier.com/locate/ijepes

A new fault location algorithm for radial distribution systems using modal analysis

Javad Sadeh [a,*], Ehsan Bakhshizadeh [b], Rasoul Kazemzadeh [b]

[a] Electrical Engineering Department, Faculty of Engineering, Ferdowsi University of Mashhad, P.O. Box 91775-1111, Mashhad, Iran
[b] Department of Electrical Engineering, Sahand University of Technology, Tabriz, Iran

ARTICLE INFO

Article history:
Received 14 September 2010
Received in revised form 14 August 2012
Accepted 29 August 2012

Keywords:
Fault location algorithm
Distribution system
Frequency spectrum
Modal analysis

ABSTRACT

In this paper, an accurate and efficient method is proposed for fault section estimation and fault distance calculation in distribution systems, based on frequency spectrum components of fault generated traveling waves. Fault occurrence in a radial distribution system generates high frequency traveling waves that can be divided into two parts. Part of them travels between fault location and substation and the other part is reflected between network junctions and substation. By identification of these two parts, the proposed algorithm determines faulted section and exact distance of fault from substation uniquely. Consequently, the main drawback of the impedance based methods which is the multiple-estimation problem is removed. In the proposed method, it is assumed that just one voltage recorder is installed at the distribution substation and additional equipments such as, fault indicators and PQ monitoring devices are also not needed to be installed in the distribution system. The simulations are carried out using ATP software and the results are processed by MATLAB software. Simulation results of various types of faults on a typical distribution system demonstrate high efficiency and accuracy of the proposed method. Effect of different influential parameters such as fault inception angle, fault resistance and load variations has also been taken into account.

1. Introduction

Fault location in distribution systems has always been of great importance to utilities for reliable power supply. It is a challenging task due to its complex nature such as having several laterals, non-symmetrical lines, highly unbalanced operation, and time-varying loads. In addition, typically in distribution systems, fault generated signals are recorded solely at the feeding substation and the location of the fault should be estimated based on these recorded data. Due to mentioned difficulties and differences the presented fault location method for transmission lines cannot be directly used for distribution systems. Thus, various methods have been exclusively proposed for fault location in distribution systems. Generally, these fault location methods can be divided into two main categories: impedance-based methods [1–7] and traveling wave-based methods [8–19]. Most of the impedance-based methods estimate the distance of the faulted point from the distribution substation based on the impedance estimation as seen from the fault locator point. In as much as the feeders of distribution system have some laterals, sub laterals and load taps, the impedance based fault location methods usually estimate several locations for a fault and cannot determine the exact fault point. It is the main common drawback of the impedance-based methods, which named multiple-estimation problem. To overcome this drawback, it is proposed to install additional apparatus such as fault indicators and PQ monitoring components in the distribution system. In the developed methods based on the traveling waves, time domain information has been usually used for determining the location of fault. Applying signal processing techniques, the high frequency components of fault generated transients are extracted and used for fault locating. In [15–17] detail coefficients of wavelet transform has been used to determine the faulted section and location. The presented method in [18] determines the location of fault based on the frequency domain analysis of the fault generated transients on branch terminals. Another method has been proposed based on the cross-correlation technique for fault location in distribution systems in [19].

In this paper an accurate fault location algorithm based on the fault generated transient is proposed. Using only one recorder device at the beginning of the main feeder to record fault generated transients in faulted phase voltage is one of the advantages of proposed method. In this method using Clark transformation, the voltage signals are first transformed from phase domain into modal domain and then frequency analysis is performed on aerial mode voltage (V_1) and ground mode voltage (V_0). Comparing the results obtained from analysis with ones on the earlier generated database, the proposed algorithm determines faulted section and distance of fault uniquely. Furthermore, the accuracy of the result can be improved to desired level by increasing the recorded data

* Corresponding author. Tel./fax: +98 5118763302.
E-mail address: sadeh@um.ac.ir (J. Sadeh).

0142-0615/$ - see front matter © 2012 Elsevier Ltd. All rights reserved.
http://dx.doi.org/10.1016/j.ijepes.2012.08.053

in the database. In order to validate the accuracy of the proposed method, a sample distribution system with several sections and laterals is simulated under ATP software and the results are processed in MATLAB. The obtained results show the accuracy and precision of the proposed method in determining the section and the location of fault.

2. Proposed fault location algorithm for radial distribution systems

When a fault happens in a distribution feeder, it causes to produce traveling waves (TWs) that travel between fault location and substation. Hence, frequency of the TW measured at the substation is directly related to the fault distance from substation. By increasing fault distance, period of TW increase and so their frequency goes down. However, for a distribution system that comprise of a main feeder and many laterals, in addition to the reflected waves from the fault location (the main components), some reflected waves from junctions also reach to substation (measuring point). These waves (which contain less energy in compared to the main components) also generate components in frequency spectrum of faulted voltages that in this paper are called subordinate components. Using Clark transformation, the faulted voltages are first transformed from phase domain into modal domain. Then frequency analysis is performed on aerial mode voltage (V_1) and ground mode voltage (V_0) to identify both main and subordinate components. Comparing the results obtained from analysis with earlier generated database, the proposed algorithm determines faulted section and distance of fault uniquely.

Because of delta connection of the secondary winding of distribution transformers, amplitude of single line to ground (SLG) fault current with respect to other fault types is lower. Hence, the amplitude of TW produced by SLG faults in comparison to other fault types is smaller considerably. In this circumstance distinction between the main and the subordinate components cannot be done precisely. Accordingly, faults are divided into two groups in this paper. The SLG faults and the other fault types. Two individual algorithms are developed for detecting the section and location of each group of fault.

2.1. Proposed technique for locating all types of fault except SLG

The proposed method is described using a sample distribution system shown in Fig. 1. This system includes a main feeder and several laterals with different lengths. The 3-phase voltages are recorded only in the substation. Fig. 2 shows the frequency spectrum of the first aerial mode of the voltage (V_1), generated by simulation of 3-phase symmetrical faults on the main feeder, locate at different distances of 6, 7, 9, and 10 km from the substation. All frequency components of the voltages in Fig. 2 are generated by reflections of high frequency transients between the fault location and the substation (main components). Fig. 2 indicates that by increasing the fault distance, frequency of the main components in voltage V_1 decreases. For instance, frequency of the first component of TW (component with maximum amplitude named dominant main component (DMC) in this paper) for 3-phase faults located at 6, 7, 9, and 10 km form the substation is 14,450, 12,720, 10,020, and 9058 Hz, respectively. Simulation results for 3-phase faults in different locations of the test system, confirm the decreasing trend of the frequency versus the increase of the fault distance. Hence this criterion can be used to calculate the exact location of the fault. Fig. 3 illustrates the dominant main component frequency (DMCF) versus distance, obtained from simulation of the 3-phase faults with 1 km distance step. Simulations of the 3-phase faults in different locations of the laterals for each path in the distribution system of Fig. 1 yield to a curve similar to Fig. 3.

Thus, by using recorded curves related to each path in a database and calculating the DMCF of V_1, exact distance of the fault can be calculated. It should be noted that in order to reach a higher accuracy for fault distance calculation, the distance step between simulated faults can be chosen as small as needed.

In addition to determination the location of fault, the faulted section in the distribution system should be identified. Analysis of various faults shows that when a fault happens on a branch, there will be one or more subordinate components in addition to the main components. As shown in Fig. 4, when a fault happens on a branch, fault-generated transients travel toward the substation. Parts of these transients are reflected from substation toward fault point (Rm waves) and the other part propagates away from substation toward the main feeder (R waves). Part of transients which are traveling between fault point and substation, generates main components in frequency spectrum (similar to Fig. 2), while the other part which are reflected between junctions and substation, produces subordinate components. As shown in Fig. 4, by closing the faulted section to the substation, number of nodes between fault point and substation decreases. The amplitude of TW reduces by passing through nodes. So, when the number of nodes between fault location and substation increases, traveling wave amplitude decreases more at the substation [17].

In Fig. 4 all of TW from Rm1–Rm6 that reaches to substation, can generate reflections R1–R5 which induce subordinate components in frequency spectrum of V_1. Researches in this field show that usually the first subordinate component has considerable amplitude in comparison to the main components in frequency spectrum of V_1. In this paper, the first subordinate component is called dominant subordinate component (DSC).

The more amplitude of TW at substation produces R waves which pass more distance over the main feeder and therefore reflect from a farther node. The farther node means increasing the

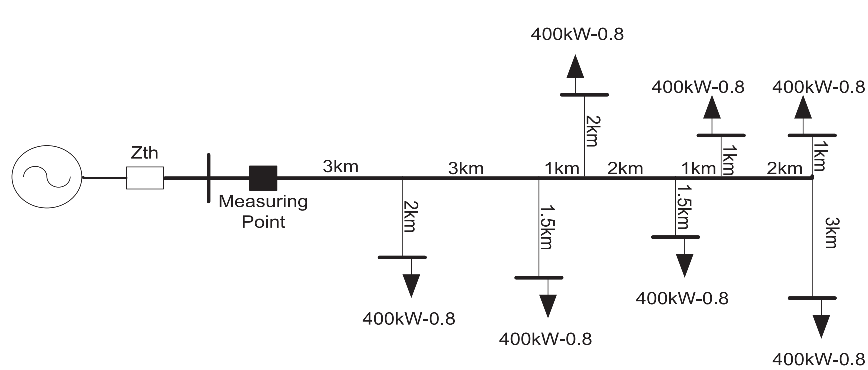

Fig. 1. Typical radial distribution system.

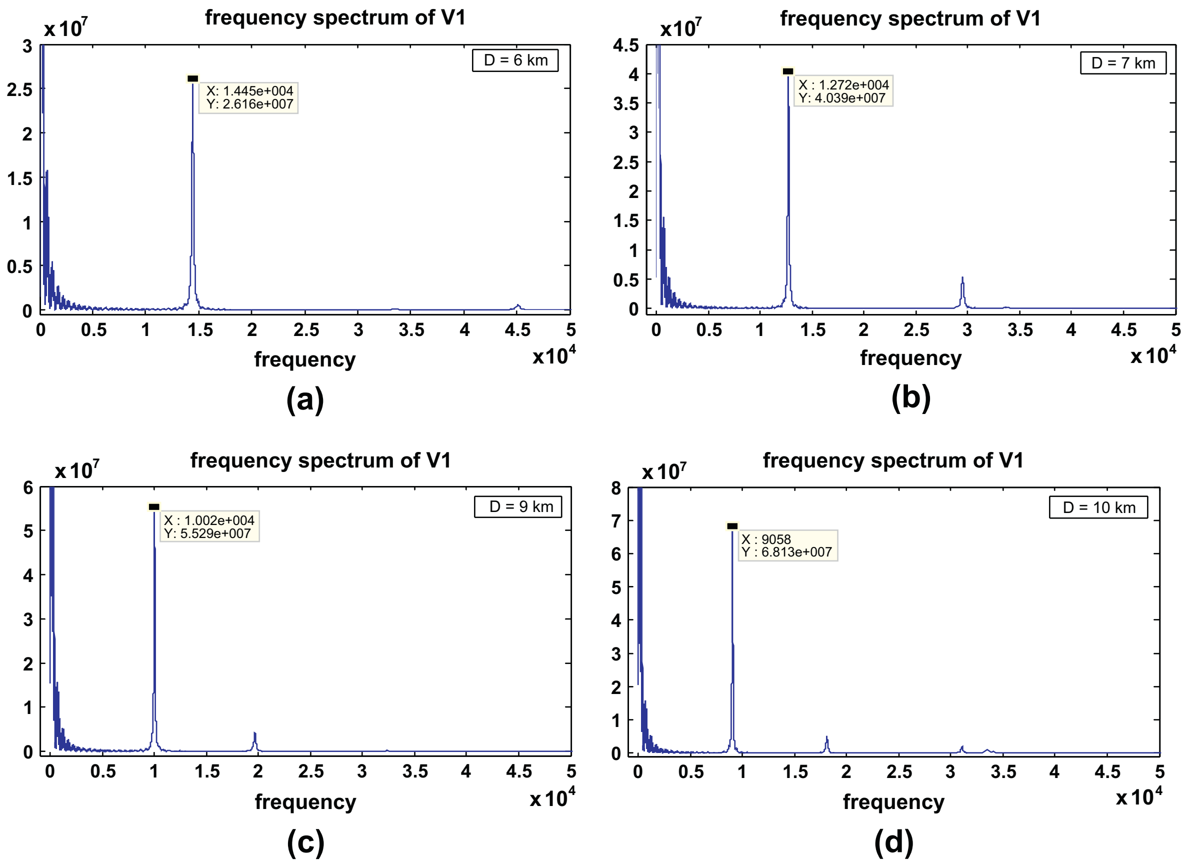

Fig. 2. Frequency spectrum of the first aerial mode of voltage V_1 at substation for 3-phase faults on the main feeder at distance of (a) 6, (b) 7, (c) 9, and (d) 10 km from substation.

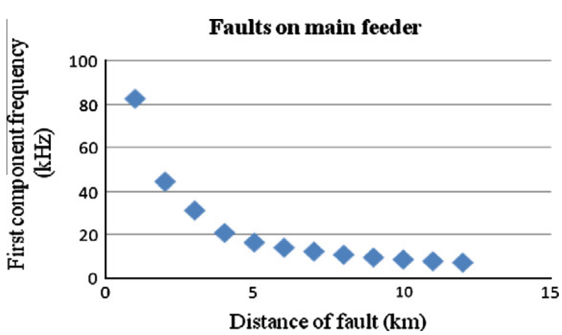

Fig. 3. Dominant main component frequency of V_1 versus different 3-phase symmetrical fault locations on the main feeder.

oscillation period and decreasing the frequency of DSC, and vice versa. Hence, it is concluded that when fault happens on farther branch regarding to substation, frequency of generated DSC increases.

Based on the above discussions, difference between the frequencies of the DSC and DMC of TW can be used to determine faulted branch. Thus *DF* is defined as follows:

$$DF = f_a - f_1 \tag{1}$$

where f_1 is the frequency of DMC and f_a is the frequency of DSC, if it is existed, otherwise f_a is chosen as the frequency of the second main component. It should be noted that faults on the main feeder

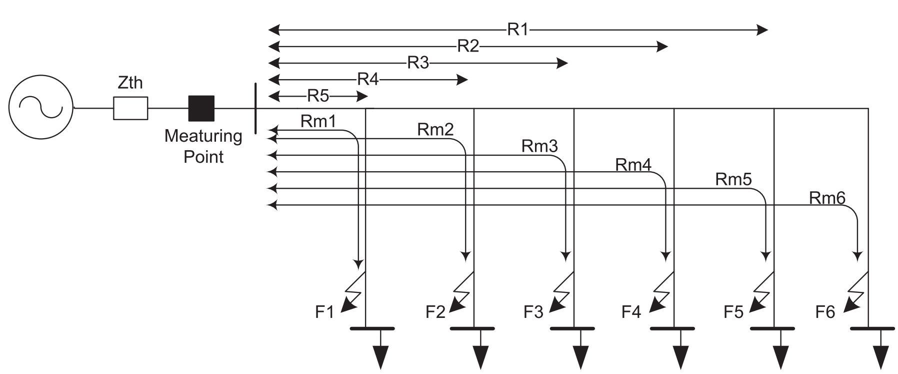

Fig. 4. Main paths of propagation of fault-generated traveling waves.

do not generate subordinate component with considerable amplitude.

To observe the trend of subordinate component, 3-phase faults are simulated on branches 1–6 in distribution system of Fig. 1, and the frequency spectrum of V_1 are shown for each fault in Fig. 5. As shown in this figure, in addition to DMCs, DSCs are also generated. Frequencies of DSCs are 4993, 6571, 7191, 10,940, 12,200, and 14,520 Hz respectively. Table 1 shows the values of *DF* for Fig. 5a–f respectively.

In Fig. 5a there are three subordinate components with considerable amplitude for faults occurred on the first branch. So first

Table 1
Increasing trend of *DF* versus increase of branch distance from the substation.

Branch	*DF* (Hz)
First branch	−22,337
Second branch	−6619
Third branch	−4499
Fourth branch	+2191
Fifth branch	+4222
Sixth branch	+7739

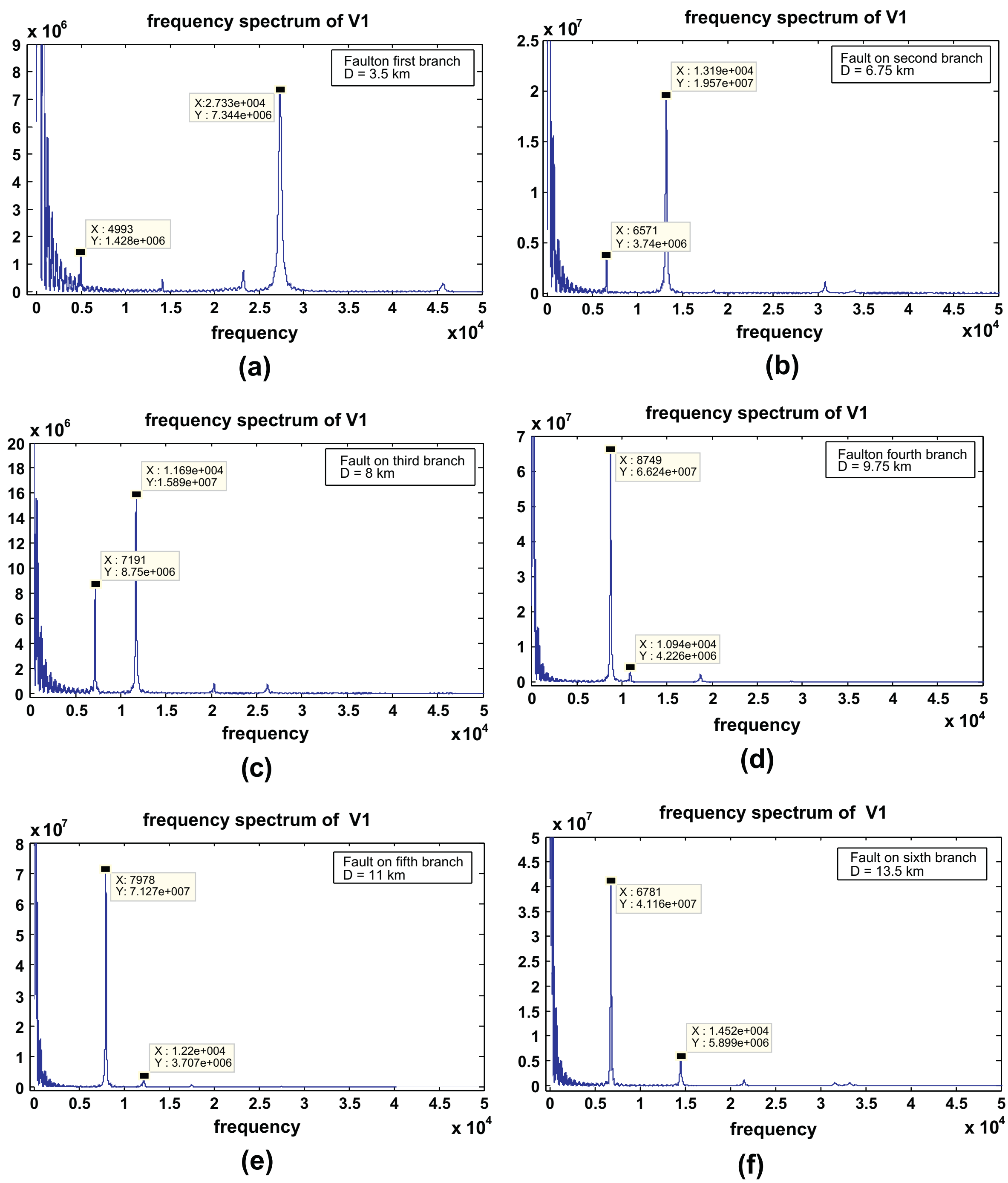

Fig. 5. Frequency spectrum of aerial mode voltage V_1 at substation for 3-phase faults on first to sixth branches with distance of (a) 3.5 km, (b) 6.75 km, (c) 8 km, (d) 9.75 km, (e) 11 km, and (f) 13.5 km from substation respectively.

subordinate component with lower frequency is picked up to calculate *DF* in Eq. (1). Table 1 indicates that by increasing the number of nodes between faulted branch and substation, the value of *DF* increases regularly.

Simulating faults in different points shows that value of *DF* along each branch is almost constant. Considering increasing trend of *DF* versus increasing the distance of faulted branch from substation, *DF* can be used as a criterion to identify faulted branch in distribution systems. So, the proposed algorithm for identification of faulted section and calculation of fault distance from substation in a distribution system can be summarized as follows:

Step 1: DMC and DSC (if any) of the TW in V_1 are identified and *DF* is calculated using Eq. (1).
Step 2: Using generated database, branches whose frequency curves contain DMCF are identified and *DF* is calculated for each branch.
Step 3: The faulted branch is identified by comparing the *DF* value for fault with the *DF* value associated with identified branches in the previous step.
Step 4: Fault distance is calculated based on the DMCF using frequency–distance curve associated with faulted branch.

Although the above mentioned results are presented for 3-phase faults, simulation results show that the frequency components in frequency spectrum of V_1, for all types of faults except SLG happened at the same positions, are identical. Hence, the extracted curves for the 3-phase faults can be used for identification of the faulted section and fault distance of all fault types except SLG.

2.2. Proposed technique for locating SLG faults

The proposed algorithm in the previous section cannot be applied to locating the SLG faults. Although grounding transformers is placed at the secondary side of sub-transmission power transformer, but due to delta connection of secondary winding, amplitude of current for SLG faults decreases significantly in comparison to the other types of fault. So, the amplitude of SLG fault generated TW, is less than the other fault types considerably and distinguishing DMCs and DSCs cannot be done precisely.

Phase voltages of fault measured at substation, for 3-phase and SLG faults at 6 km on the main feeder of Fig. 1 are shown in Fig. 6. Simulating of SLG faults in different points shows that frequency spectrum of the first aerial mode voltage (V_1) and the ground mode voltage (V_0) are the same, but amplitude of frequency components of V_0 is higher than V_1. So, in this paper, application of ground mode voltage (V_0) is proposed for locating SLG faults. Fig. 7 shows frequency spectrum of V_1 and V_0 for a SLG fault at 6 km on the main feeder. Results of simulations show that frequency spectrum of modal voltages are identical for SLG faults on the branches and the main feeder. It should be noted that decrement in frequency versus increasing in the fault distance from substation is still a valid fact for all paths of the distribution system, but rate of the frequency decrease for faults on a branch is faster than that of faults on the main feeder. So, frequencies for the faults on the branches or on the main feeder with the same distance from substation are not equal. Therefore, if two SLG faults are occurred at point A1 on a branch and point B1 on the main feeder with the same distance from the substation, frequency components of V_0 for fault at A1 is less than that of fault at B1. On the other hand, if two SLG faults are happened at points A2 and B2, equally distant from the substation, but A2 is located on a branch farther than B2, frequency components of V_0 for fault at A2 is less than that of fault at B2. So the frequency difference (*DF*) in the frequency spectrum of V_0 can also be used as a criterion for identification of faulted section. Based on the proposed criterion, by increasing the distance of the faulted branch from substation, *DF* values are decreased for fault locations with the same DMC frequencies.

Therefore, the proposed algorithm for identifying the faulted section and calculation of the SLG fault distance from substation is summarized as follows:

Step 1: The value of *DF* in frequency spectrum of V_0 is calculated.
Step 2: Using generated database, branches whose frequency curves contain DMC frequency of V_0 is identified.
Step 3: *DF* values due to fault and identified branches in step 2 are compared to identify faulted section.
Step 4: Fault distance is calculated based on the DMC frequency using frequency–distance curve of associated faulted section.

3. Simulation results

In order to evaluate the accuracy of the proposed algorithm, distribution system of Fig. 1 is simulated using ATP software. Frequency dependent parameter model is used for modeling the lines. The conductor of main feeder is Lynx and the branch ones are Mink. Sampling frequency is chosen to be 300 kHz. The studied system is simulated under various types of faults along different

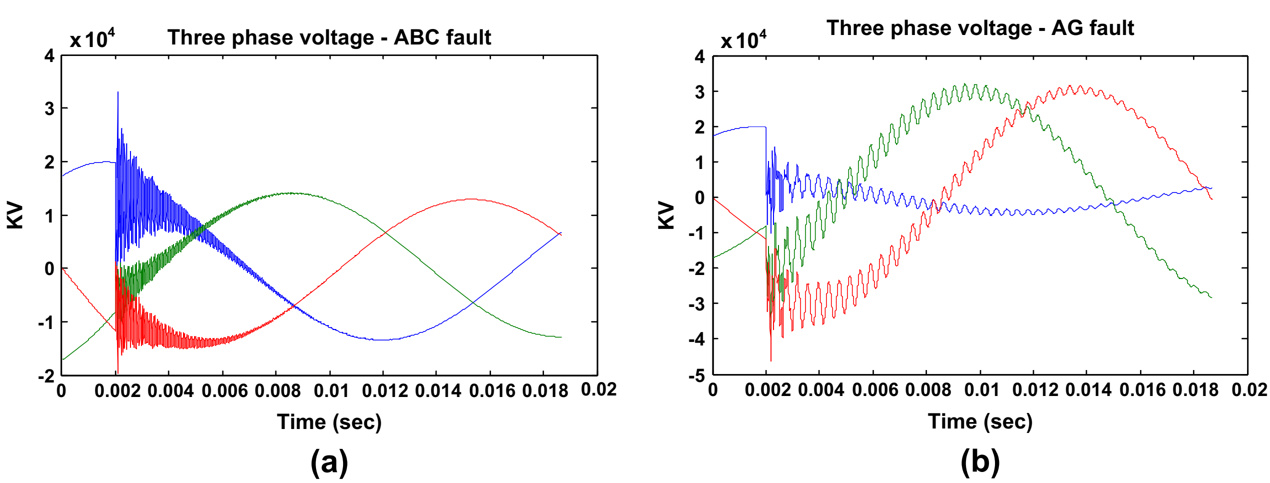

Fig. 6. 3-phase voltages for (a) 3-phase fault and (b) single phase fault on the main feeder at 6 km.

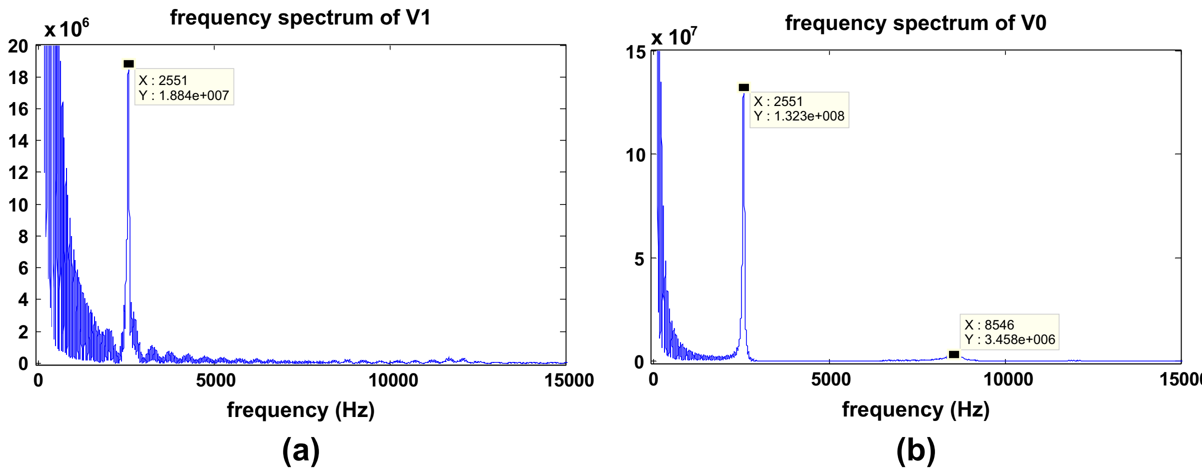

Fig. 7. Frequency spectrum of V_1 and V_0 for SLG fault on the main feeder at 6 km.

line segments and the results are presented in the following subsections.

3.1. Simulation of all types of fault except SLG

To investigate the performance of the proposed algorithm, six multiple-phase faults have been simulated on sample system of Fig. 1. These are as follows:

- *Fault 1*: ABCG fault on the main feeder, 2.1 km far from substation.
- *Fault 2*: ABG fault on the first branch, 3.75 km far from substation.
- *Fault 3*: AB fault on the second branch, 7.1 km far from substation.
- *Fault 4*: ABCG fault on the third branch, 7.27 km far from substation.
- *Fault 5*: ACG fault on the fourth branch, 10.24 km far from substation.
- *Fault 6*: AC fault on the fifth branch, 10.6 km far from substation.

The obtained results from simulation of these faults are shown in Table 2. The error of the fault location is calculated by the following equation:

$$\text{Error} = \frac{|D_{est} - D_{real}|}{L} \times 100 \quad (2)$$

where D_{est} and D_{real} represent the estimated and actual fault location, respectively, and L denotes the total line length. In this table, the result of fault section identification and distance calculation using the proposed algorithm in Section 2.1 are presented. As shown in this table, the section of all considered faults is determined correctly and the precision of the proposed fault locating algorithm is high in such a way that the error is kept below 0.6%.

3.2. Simulation of SLG faults

To investigate the accuracy of the proposed algorithm, six single phase faults have been simulated on the sample system of Fig. 1. The fault positions are as follows:

- *Fault 1*: SLG fault (AG) on the main feeder, 9.75 km far from substation.
- *Fault 2*: SLG fault (AG) on the first branch, 3.75 km far from substation.
- *Fault 3*: SLG fault (AG) on the second branch, 6.8 km far from substation.
- *Fault 4*: SLG fault (AG) on the third branch, 7.27 km far from substation.
- *Fault 5*: SLG fault (AG) on the fourth branch, 9.9 km far from substation.
- *Fault 6*: SLG fault (AG) on the fifth branch, 10.75 km far from substation.

The results presented in Table 3 indicate that the proposed algorithm has an acceptable performance with maximum percentage error of 0.25%.

3.3. Effect of fault resistance

Amplitude of frequency component on V_1 and V_0 decreases when fault resistance exists. In other words, peak value of

Table 2
Results of fault section estimation and location for multiple phase faults.

Fault no.	DMCF (Hz)	DSCF (Hz)	*DF* (Hz)	*DF* value for branches in distribution system which have the same DMCF as fault point						Estimated section	Estimated fault location (km)	Error (%)
				Main feeder	Branches							
					First	Second	Third	Fourth	Fifth			
1	42,650	109,300	**66,650**	**66,750**	–	–	3325	4241	–	Main feeder	2.092	0.067
2	26,240	4853	**−21,387**	43,920	**−21,380**	–	–	–	–	First branch	3.822	0.60
3	12,760	6299	**−6461**	16,780	–	**−6415**	–	–	–	Second branch	7.108	0.067
4	12,330	8044	**−4286**	15,330	–	–	**−4207**	–	–	Third branch	7.266	0.03
5	7990	10,820	**2830**	8200	–	–	–	**2860**	7220	Fourth branch	10.23	0.083
6	8413	12,800	**4387**	8507	–	–	–	2477	**4407**	Fifth branch	10.61	0.083

Table 3
Results of fault section estimation and location for single line to ground (SLG) faults.

Fault no.	First component's frequency in V_0 (Hz)	*DF* (Hz)	*DF* value for locations in distribution system which have the same first component's frequency as fault point						Estimated section	Estimated fault location (km)	Actual fault location (km)	Error (%)
			Main feeder	Branches								
				First	Second	Third	Fourth	Fifth				
1	2403	**4107**	**4084**	–	–	3325	4241	–	Main feeder	9.78	9.75	0.25
2	2567	**6455**	6209	**6426**	–	–	–	–	First branch	3.78	3.75	0.25
3	2496	**5632**	5249	–	**5648**	–	–	–	Second branch	6.81	6.80	0.05
4	2497	**5391**	5331	6342	5655	**5415**	–	–	Third branch	7.29	7.27	0.16
5	2383	**4068**	3877	–	–	3172	**4045**	–	Fourth branch	9.88	9.90	0.17
6	2354	**3739**	3616	–	–	–	3677	**3744**	Fifth branch	10.74	10.75	0.08

Table 4
Results of fault location when the fault resistance is 15 Ω.

Fault no.	First component's frequency in V_0 (Hz)	*DF* (Hz)	Estimated fault location (km)	Error (%)
1	2390	4121	9.79	0.33
2	2558	6466	3.85	0.83
3	2497	5630	6.815	0.13
4	2497	5390	7.34	0.58
5	2380	4073	9.88	0.67
6	2362	3731	10.65	0.83

Table 5
Fault location results for different fault inception angles.

Fault no.	Fault inception angle (°)	First component's frequency in V_0 (Hz)	Estimated fault location (km)	Error (%)
1	90	2403	9.78	0.25
	45	2402	9.76	0.08
	30	2402	9.82	0.55
2	90	2567	3.78	0.25
	45	2590	3.69	0.50
	30	2585	3.81	0.48

Table 6
Results of fault location in case of 30% load variations.

Fault no.	First component's frequency in V_0 (Hz)	*DF* (Hz)	Estimated fault location (km)	Error (%)
1	2393	4117	9.79	0.33
2	2563	6461	3.83	0.67
3	2489	5639	6.78	0.17
4	2490	5398	7.36	0.75
5	2375	4076	9.87	0.25
6	2344	3748	10.86	0.92

frequency components attenuates. As the proposed algorithm is developed based on the frequency, not based on the amplitude, changes in amplitude of frequency component do not affect performance of the proposed algorithm considerably. Results for six SLG faults in the previous section with fault resistance of 15 Ω which are shown in Table 4, confirm this fact. The maximum percentage of error in these conditions is 0.83%.

3.4. Effect of fault inception angle

Because proposed algorithm works based on the frequency components of traveling waves, changes in voltage angle, which lead to frequency spectrum amplitude changes, have no considerable effect on the algorithm performance. In Table 5 the results of simulation of faults 1 and 2 with different fault inception angles are summarized. The maximum error for these conditions is 0.55%.

3.5. Effect of load variations

To investigate the performance of the proposed algorithm in situation of load variations, load impedance for each branch is changed by 30%. Table 6 shows results of simulations using the proposed algorithm.

The presented results in Tables 2–6 are obtained based on the recorded data in database for simulation faults located with step distance of 1 km on the main feeder and 0.5 km on the branches. Obviously, reducing these distance steps would result to better accuracy of the proposed algorithm.

3.6. Comparing the proposed method accuracy to recent presented methods

In order to demonstrate the accuracy of the proposed fault location method, some of presented papers in this topic are examined in respect to the claimed percentage of error. The maximum reported errors are 2.76% in [2], 7.3% in [3], 10.97% in [4], 1.58% in [5], 3.17% in [9], and 10.65% in [13]. However, the maximum error in the proposed method is kept below 1%. Comparing the reported errors and that of the proposed method, it can be concluded that the presented method in this paper has high accuracy, which is a salient advantage of the proposed method.

4. Conclusion

A new technique for fault location in distribution systems is proposed based on the frequency spectrum components of fault-generated traveling waves. In the proposed method, by constructing an offline database and comparing the obtained data from analyzing the fault generated voltage with the data gathered in the database, it can determine the section and the distance of fault accurately. It is worth noting that the proposed method does not need any data from the additional equipments in the distribution system and just use from voltage signal at the beginning of the feeder. Additionally, using voltage signal has some advantages over current one. Using the current signals may be associated with a decrease in fault locating accuracy level caused by existence of significant DC component and saturation of current transformer (CT). Simplicity and possibility of improving the accuracy of the results by extending the offline database are the main advantages of the proposed method. Performance of the proposed algorithm is evaluated by simulation of various types of faults on a sample distribution system with several branches. Analyzing various fault types under different conditions such as load variations, fault inception angle and fault resistance confirms the high accuracy of the proposed method.

References

[1] Mora-Florez J, Melendez J, Carrillo-Caicedo G. Comparison of impedance based fault locations methods for power distribution systems. Electr Power Syst Res 2008;78(4):657–66.
[2] Filomena AD, Resener M, Salim RH, Bretas AS. Fault location for underground distribution feeders: an extended impedance-based formulation with capacitive current compensation. Int J Electric Power Energy Syst 2009;31:489–96.
[3] Aslan Y, Ture S. Location of faults in power distribution laterals using superimposed components and programmable logic controllers. Int J Electric Power Energy Syst 2011;33:1003–11.
[4] Salim RH, Resener M, Filomena AD, Caino de Oliveira KR, Bretas AS. Extended fault-location formulation for power distribution systems. IEEE Trans Power Deliv 2009;24(2):508–16.
[5] Salim RH, Salim KCO, Bretas AS. Further improvements on impedance-based fault location for power distribution systems. IET Gener Trans Distrib 2011;5(4):467–78.
[6] Ngu EE, Krishnathevar R. Generalized impedance-based fault location for distribution systems. IEEE Trans Power Deliv 2012;27(1):449–51.
[7] Liao Y. Generalized fault-location methods for overhead electric distribution systems. IEEE Trans Power Deliv 2011;26(1):53–64.
[8] Ngu EE, Ramar K. A combined impedance and traveling wave based fault location method for multi-terminal transmission lines. Int J Electric Power Energy Syst 2011;33:1767–75.
[9] Borghetti A, Bosetti M, Nucci CA, Paolone M. Continuous-wavelet transform for fault location in distribution power networks: definition of mother wavelets inferred from fault originated transients. IEEE Trans Power Syst 2008;23(2):380–8.
[10] Shu H, Wang X, Xia Q, Wu Q, Tian X. A fault location method of traveling wave for distribution network with only two-phase current transformer using artificial neutral network. In: 3rd International congress on image and signal processing (CISP2010); 2010. p. 2942–5.
[11] Kang M, Bo Z. Based on the distribution network fault location simulation of wavelet modulus maxima. In: The international conference on advanced power system automation and protection (APAP), China; 2011. p. 1517–20.
[12] Wang Y, Zeng X, Qin X, Zhao Zh, Pan H. HHT based single terminal traveling wave fault location for lines combined with overhead-lines and cables. In: International conference on power system technology (PowerCon '2010), China; 2010.
[13] Pourahmadi-Nakhli M, Safavi AA. Path characteristic frequency-based fault locating in radial distribution systems using wavelets and neural networks. IEEE Trans Power Deliv 2011;26(2):772–81.
[14] Lin X, Zhao F, Wu G, Li Zh, Weng H. Universal wave front positioning correction method on traveling-wave-based fault-location algorithms. IEEE Trans Power Deliv 2012;27(3):1601–10.
[15] Evrenosoglu CY, Abur A. Fault location in distribution systems with distributed generation. In: 15th Power system computation conference (PSCC'05), Session 10 Paper 5, Liege, Belgium, August 2005.
[16] Nouri H, Wang C, Davies T. An accurate fault location technique for distribution lines with tapped loads using wavelet transform. In: Proc IEEE power tech porto, September 2001. p. 10–3.
[17] Magnago FH, Abur A. A new fault location technique for radial distribution systems based on high frequency signals. IEEE Power Eng Soc 1999;1:426–31. 18–22 July 1999.
[18] Borghetti A, Corsi S, Nucci CA, Paolone M, Peretto L, Tinarelli R. On the use of continuous-wavelet transform for fault location in distribution power systems. Int J Electric Power Energy Syst 2006;28:608–17.
[19] Thomas DWP, Carvalho RJ, Pereira ET. Fault location in distribution systems based on traveling waves. In: Proc IEEE power tech, Bologna, June 2003.